**Proceedings of the ASME 2011 Power Conference (POWER 2011)**
**and the International Conference on Power Engineering 2011 (ICOPE-11)**
**July 12-14, 2011, Denver, Colorado, USA**

# JSME-50

# A LIQUID-PISTON STEAM ENGINE

**Shinichi Yatsuzuka**
DENSO CORPORATION
**Kariya, Aichi, Japan**

**Yasunori Niiyama**
DENSO CORPORATION
**Kariya, Aichi, Japan**

**Kentarou Fukuda**
DENSO CORPORATION
**Kariya, Aichi, Japan**

**Yasumasa Hagiwara**
DENSO CORPORATION
**Kariya, Aichi, Japan**

**Kazutoshi Nishizawa**
DENSO CORPORATION
**Kariya, Aichi, Japan**

**Naoki Shikazono**
THE UNIVERSITY OF TOKYO
**Tokyo, Japan**

## ABSTRACT

Reduction of global carbon dioxide emissions is one of the most critical challenges for realizing sustainable society. In order to reduce carbon dioxide emissions, energy efficiency must be improved. Waste heat recovery with external combustion engine is expected to be one of the promising technologies for efficient energy utilization. However, the temperature of waste heat is getting lower with the progress of energy technologies. For example, in Japan which is known as one of the most energy-efficient countries in the world with advanced technologies such as cogeneration and hybrid automobiles, total amount of disposed heat below 300 °C is as much as 10% of the total amount of primary energy supply. Conventional external combustion engines, such as Stirling, thermoacoustic[1] and steam engines[2] show significant decrease in their efficiency at low temperatures below 300 °C. Utilization of high-temperature heat sources, however, requires relatively expensive materials and advanced processing technologies to achieve high reliability.

In order to overcome these issues, a novel liquid-piston steam engine is developed, which achieves high efficiency as well as high reliability and low cost using low temperature heat below 300 °C. Present liquid-piston steam engine demonstrated a thermal efficiency of 12.7% at a heating temperature of 270 °C and a cooling temperature of 80 °C, which was about 40% of the Carnot efficiency operating at same temperatures. The liquid-piston steam engine operated even with wet steam, without requiring steam to be superheated. This low temperature operation yielded relatively little deformation of components, which leads to high reliability of the engine. In addition, present liquid piston engine can achieve both high efficiency and low cost compared to conventional external combustion engines, because it has only one moving part whereas both Stirling and Rankin engines have at least two moving parts.. The developed liquid piston engine is thus expected to possess large possibility of recovering energy from waste heat.

## INTRODUCTION

Primary energy sources, such as fossil fuels, solar and biomass are finally converted to heat when they are utilized in industry, transportation and consumer sectors. It is difficult to recycle heat losses from mechanical friction and power generators. However, almost one-half of the waste heat is dissipated as exhaust gas or coolant heat, which can be recycled with less difficulties. Waste heat recovery with external combustion engine is thus expected to be one of the promising technologies for efficient energy utilization.

For example, total amount of disposed heat as exhaust gas or coolant heat below 300 °C is as much as 10% of the total amount of primary energy in Japan. Conventional external combustion engines, such as Stirling, thermoacoustic or steam engines show significant decrease in their efficiency at low-temperatures below 300 °C. In this paper, we propose a novel liquid-piston steam engine, which achieves high efficiency at low temperatures below 300 °C as well as high reliability and low cost. In addition, the thermal efficiency of this engine is evaluated by experiment and calculation.

## STRUCTURE AND PRINCIPLE OF OPERATION OF THE LIQUID-PISTON STEAM ENGINE

Figure 1 shows the structure and operation principle of the proposed liquid-piston steam engine. The engine is composed of heating section, cooling section to condense steam, and solid piston to extract work.

The working fluid, which is water in this study, is called “liquid piston”, because it moves in synchronization with the solid piston. Water entering the heating section boils and

vaporizes to yield high pressure, which pushes the liquid surface in a downward direction (Fig. 1). Only vaporization takes place when the gas-liquid interface is in the heating section, because the cooling section is filled with water. After the gas-liquid interface passes the top dead point, continuous vaporization of the remained water in the heating section maintains high pressure which further pushes down the piston. When the gas-liquid interface is pushed down into the cooling section, steam starts to condensate. When the liquid piston is near the bottom dead point, only condensation takes place because there is no liquid in the heating section. As the liquid piston passes the bottom dead point, the inertial energy of the flywheel pushes the piston upward to reduce the volume of the cylinder. Figure 2 illustrates an ideal cycle diagrams for the case with boiling pressure of 5 MPa and condensing pressure of 0.05 MPa.

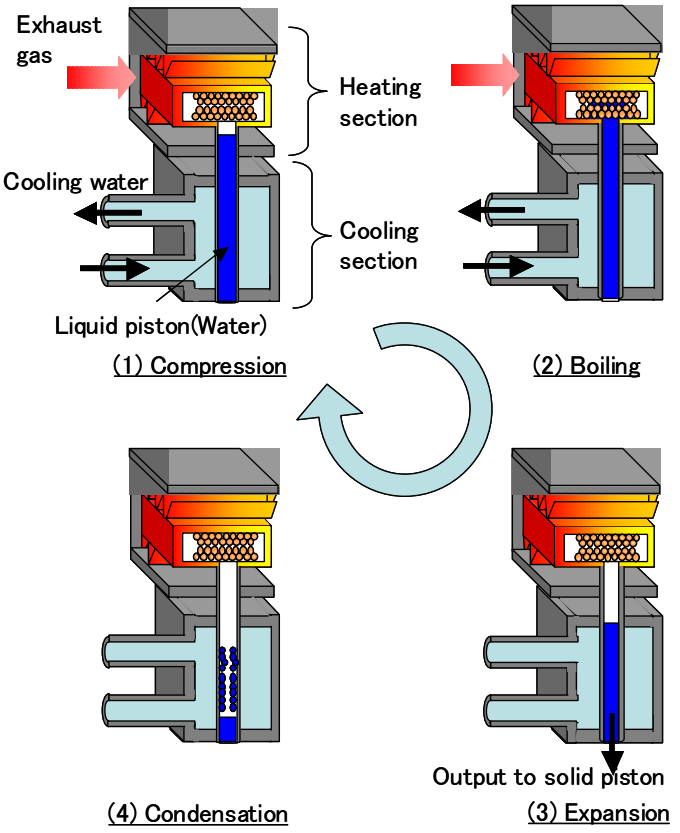


Fig. 1 Structure and operation of the liquid-piston steam engine

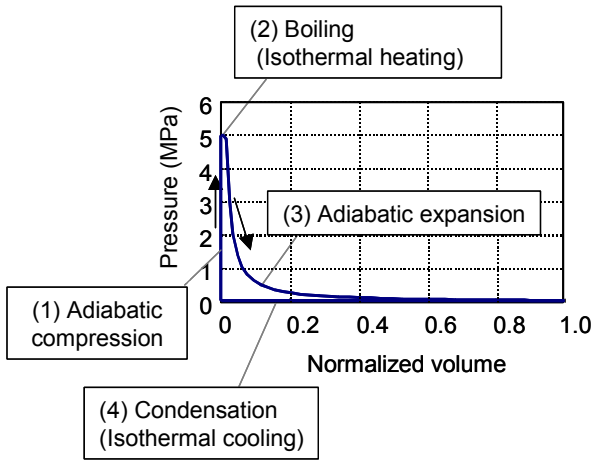


(a) *P-V* diagram

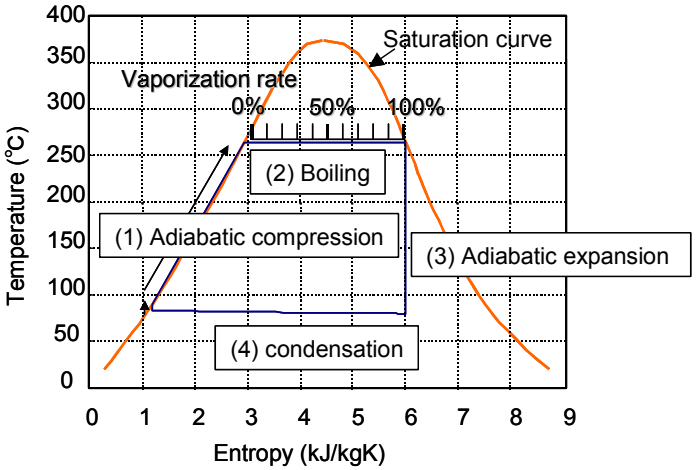


(b) *T-S* diagram

Fig. 2 Ideal cycle diagrams of the liquid-piston steam engine.

## DETAILED DESIGN OF THE LIQUID-PISTON STEAM ENGINE

The liquid-piston steam engine is a thermal reciprocating engine. A so-called thermal transport loss accompanies with this type of thermal engines. In the liquid-piston steam engine, the water heated in the boiling cycle that has not reached the boiling point moves back to the cooling section as part of the liquid-piston during the expansion period. And this results in thermal transport loss. The efficiency of the engine increases as the amount of water entering the heating section is reduced, because this lowers the thermal transport loss. A highly efficient sintered metal evaporator with high boiling heat transfer coefficient[3] is developed, which can vaporize water rapidly during the boiling period.

The sintered metal was moulded using plasma-sintering method. A small pressure was applied to spherical copper granules with almost uniform diameter, which were arranged in a close-packed hexagonal lattice. This porous structure enables

liquid and steam to flow, and at the same time works as high performance fins.

The following assumptions are introduced in order to calculate thermal efficiency of the cycle.

Firstly, boiling heat flux is assumed to follow Kutateladze's equation[4]:

$$q(t) = 3.12\times10^{-11}\times\lambda^{3.3}\times\left(\frac{P}{\nu_L h_{fg}\rho_V\sigma}\right)^{2.3}\times\left(\frac{\sigma}{g(\rho_L-\rho_V)}\right)^{0.67} \times \mathrm{Pr}^{1.17}\times(T_W - T_S(t)) \quad , (1)$$

where $q$, $\lambda$, $P$, $\sigma$, $\rho$, $h_{fg}$, $\nu$, $g$, Pr and $T$ represent heat flux, thermal conductivity, pressure, surface tension, density, latent heat, kinematic viscosity, gravitational acceleration, Prandtl number and temperature, respectively. The subscripts $L$, $v$, $w$ and $s$ represent liquid, vapor, wall and saturated steam.

The second assumption is that the phase transition occurs at the saturation temperature, and superheat and subcool are not considered. The temperature distribution of water was thus obtained by analysing the unsteady thermal conduction equation (2), with the heat flux equation (1) as its boundary condition:

$$q(t)A(t) = -\lambda_L A(t)\left.\frac{\Delta T}{\Delta y}\right|_{y=0} \quad , (2)$$

where $A$ represents the area of thermal conduction, which is the contact area between the liquid piston and the heat exchanger, and $y$ represents the distance from the surface of cylindrical flow path.

Thirdly, it is assumed that the gas phase can be recognized as an ideal gas:

$$PV = \frac{m_g}{M}RT \quad , (3)$$

where $m_g$ and $M$ represent the amount of steam generated and molecular weight.

Fourthly, the performance of cooling (condensation) is assumed to be sufficiently high, and thus the thermal resistance of condensation is assumed to be zero.

Fifthly, the sintered metal evaporator is modelled as bundled cylinders as shown in Fig. 3.

Sixthly, generated steam can move to the steam reservoir immediately, which corresponds to the assumption of spatially uniform pressure in the system.

Seventhly, the temperature of the sintered metal is assumed to be constant during the whole cycle.

The detailed calculation was carried out under these assumptions. Figure 4 shows the flow chart of the calculation procedure. The cycle is divided into 100 intervals. The thickness of sintered metal is 0.5 mm, the operation frequency is 3 Hz which is due to the constraint of boiling thermal conduction, the cylinder capacity is 7 cc and the amount of water able to enter the heating section is 0.1cc. The cooling section temperature is 80 °C assuming automobile coolant.

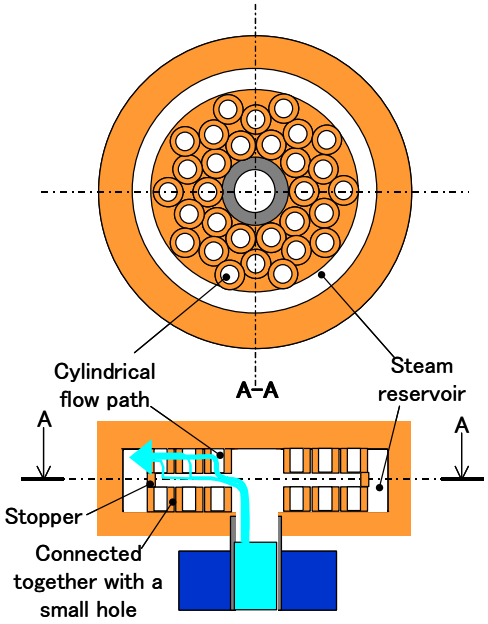


Fig. 3 Model for the sintered metal evaporator.

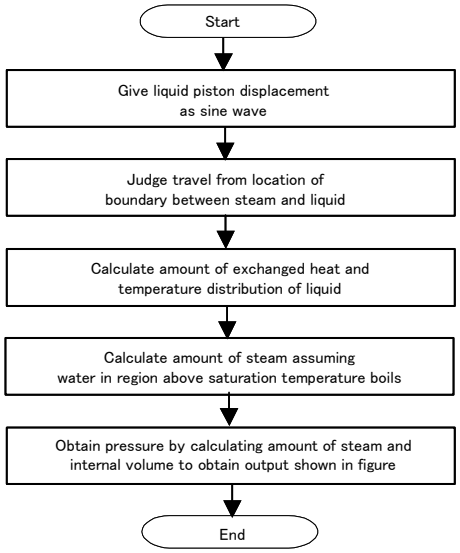


Fig. 4 Flow chart of the calculation procedure.

Figure 5 shows the thermal efficiencies of the cycle against operating temperature with different pore diameters of the sintered metal. The calculation was carried out for three cases: (a) a case with constant entropy adiabatic expansion where no condensation takes place, (b) a case that 30% of vapor condenses during expansion period and (c) a case with 50% condensation. The thermal efficiencies increase as operating temperature increases, following the same trend with the Carnot efficiency curve. Figure 6(a) shows the *T-S* diagram with different pore diameters at an operating temperature of 270 °C. Figure 6(b) shows the effect of condensation ratio during the expansion period with pore diameter of 20 μm. The vaporization ratio was only 26 % with a channel hydraulic

diameter of 200 μm, and the thermal efficiency was only 9.5 % (29 % of the Carnot efficiency) due to the thermal transport loss. On the other hand, the vaporization rate rose more than 80 % with a pore diameter of 20 μm. This lead to the reduction of thermal transport loss, thereby achieving an efficiency over 25% (80 % of the Carnot efficiency). Even if 50 % of the vaporized steam condensed during the expansion cycle, a thermal efficiency over 10 % can be expected at an operating temperature of 270 °C.

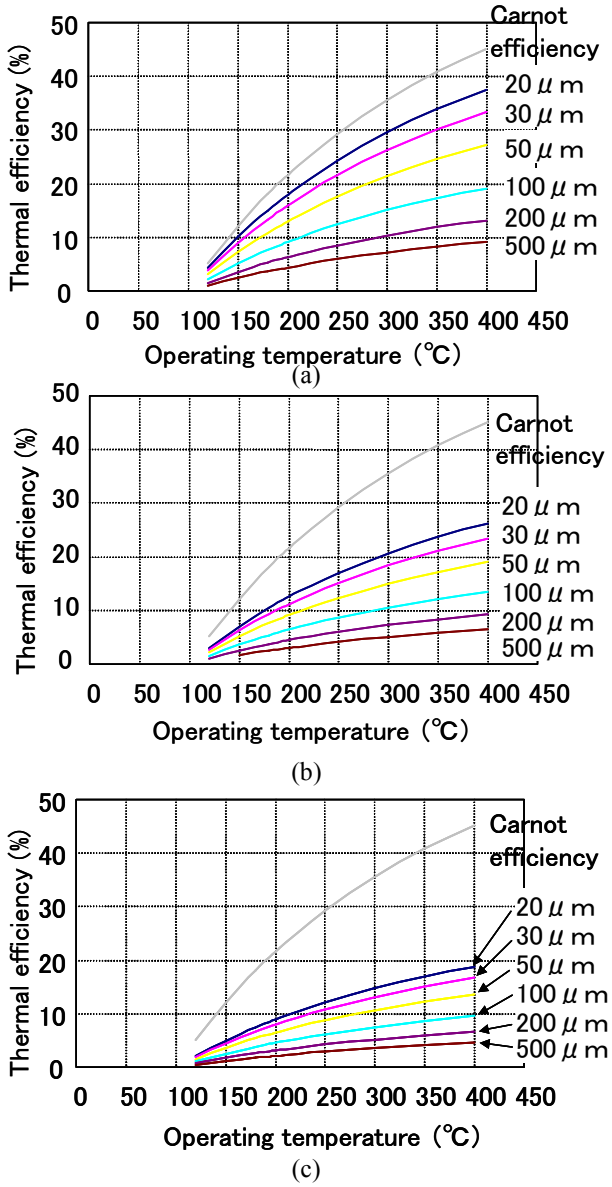


Fig. 5 Thermal efficiencies of the cycle against operating temperature with different pore diameters of the sintered metal (a) Reversible adiabatic expansion during the expansion period, (b) 30% of vapor condenses during expansion period and (c) 50% of the vaporized steam is condensed.

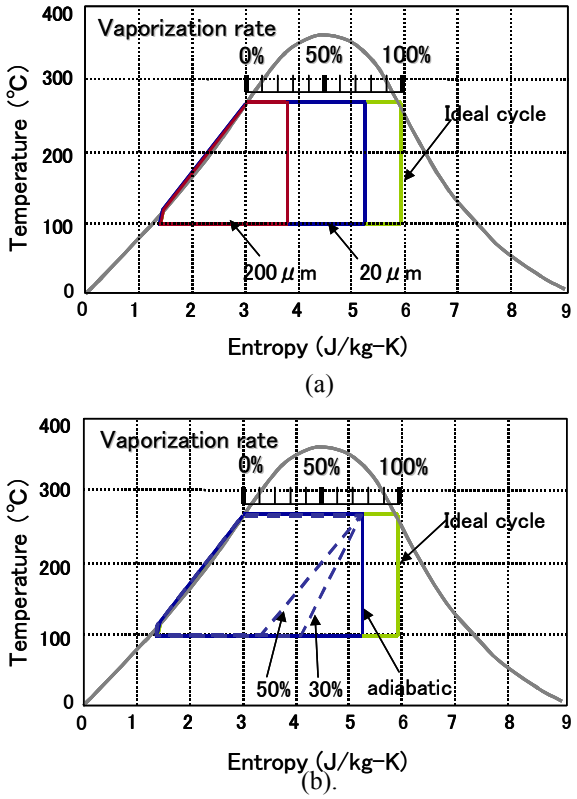


Fig. 6 *T-S* diagrams of the cycle. (a) Effect of pore diameter with reversible adiabatic expansion during the expansion period, and (b) Effect of condensation rate during the expansion period.

## EXPERIMENTAL VERIFICATION

We experimentally verified the efficiency of the liquid piston steam engine with two prototype evaporators, one with sintered metal and the other without sintered metal. The hydraulic diameter of the pores in the sintered metal was 20 μm, and that of the hollow channel was 200 μm. Figure 7 shows the structures of the heating sections. Figure 8 shows the experimental setup. The experimental setup is composed of heating section, cooling section, water for the liquid piston and an expansion device. Engine power and its thermal efficiency are calculated from the measured *P-V* diagram and electric heater input. Equations (4) and (5) were used for this calculation:

$$W = \oint P A_P dX \quad , (4)$$

$$\eta = W / Q_e \quad , (5)$$

where, $W$, $A_P$ $X$ and $Q$e represent work from *P-V* diagram, cross sectional area of the piston, piston position and electric heater input power, respectively.

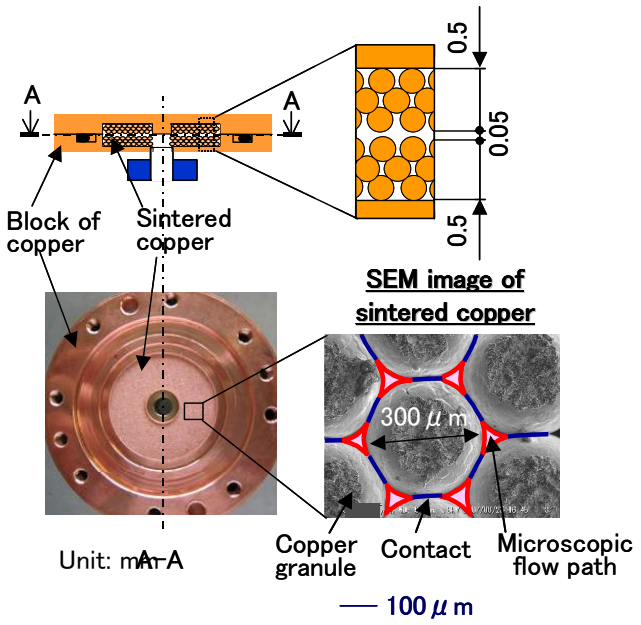


(a)

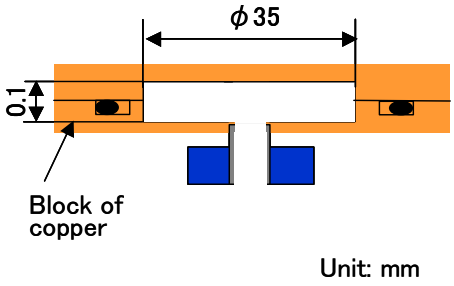


(b)

Fig. 7 Structures of the evaporators. (a) Sintered metal and (b) hollow channel evaporators.

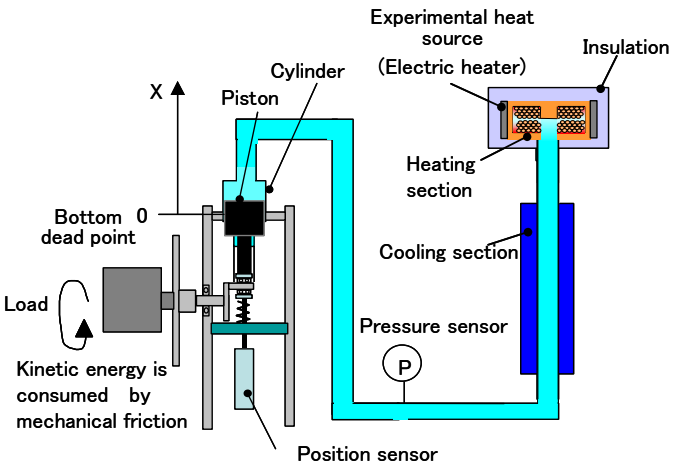


Fig. 8 Experimental setup.

Figure 9 shows the measured thermal efficiency. The calculated results for hydraulic diameters of 20 and 200 μm are also plotted in the figure. The sintered metal-type evaporator showed higher efficiency than the hollow channel evaporator at all temperatures. The thermal efficiency was 12.7% at an operating temperature of 272 °C, which was approximately 40% of the Carnot efficiency. The experimental results exhibited values close to the calculated values in the case in which the condensation rate was 50% during the expansion period. This measured efficiency value is much higher than those of thermoelectric devices and thermoacoustic engines whose reported conversion efficiencies are less than 10% operating between 270 °C and 80 °C[1]. Figure 10 shows the pressure profile for sintered metal-type evaporator. Figures 11 and 12 show *P-V* and *T-S* diagrams, respectively. Figure 12(b) shows the cycle diagram for the hollow channel evaporator. The higher efficiency of the sintered metal evaporator can be attributed to the higher vaporization rate. The slope of the measured pressure curve during expansion is smaller than ideal adiabatic expansion line as shown in Fig. 11. This is considered to be due to the vaporization of remaining water in the heating section. In addition, the temperature decrease observed during the boiling period shown in Fig. 12(a) can be attributed to the temperature drop of the sintered metal.

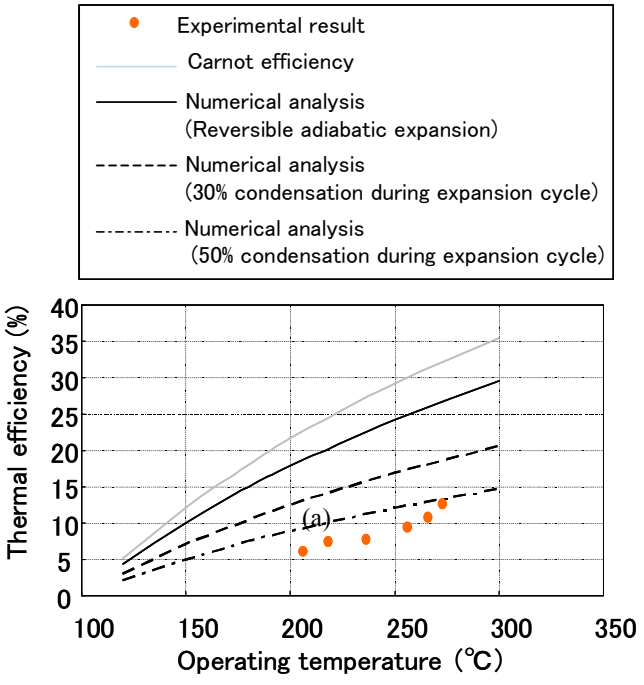


(a)

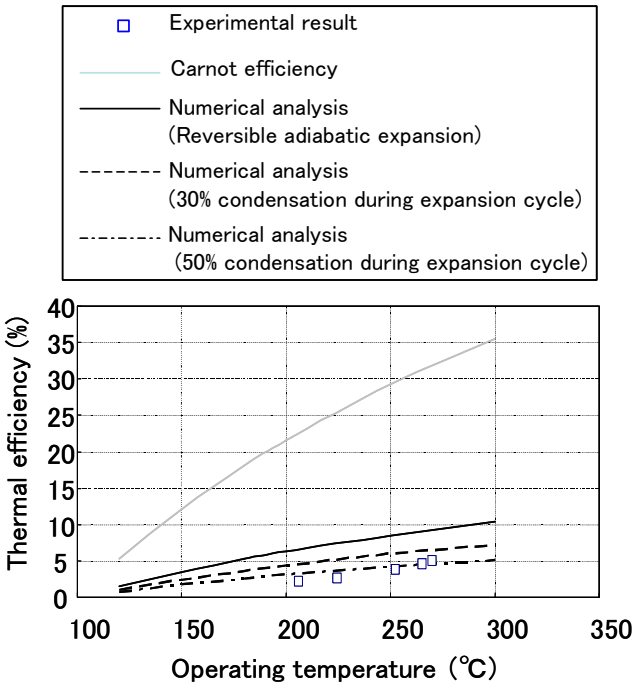


(b)

Fig. 9 Measured thermal efficiency. (a) Sintered metal and (b) hollow channel evaporators.

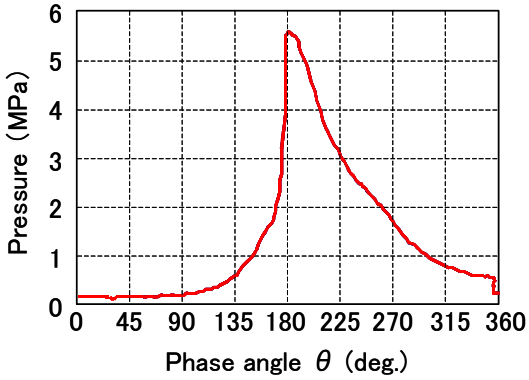


Fig. 10 Pressure profile for the sintered metal-type evaporator.

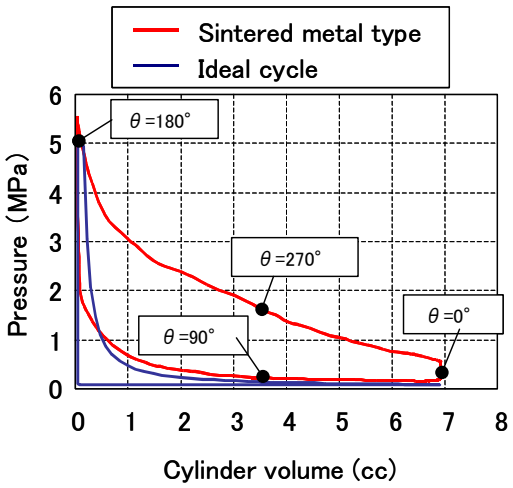


Fig. 11 *P*- *V* diagram.

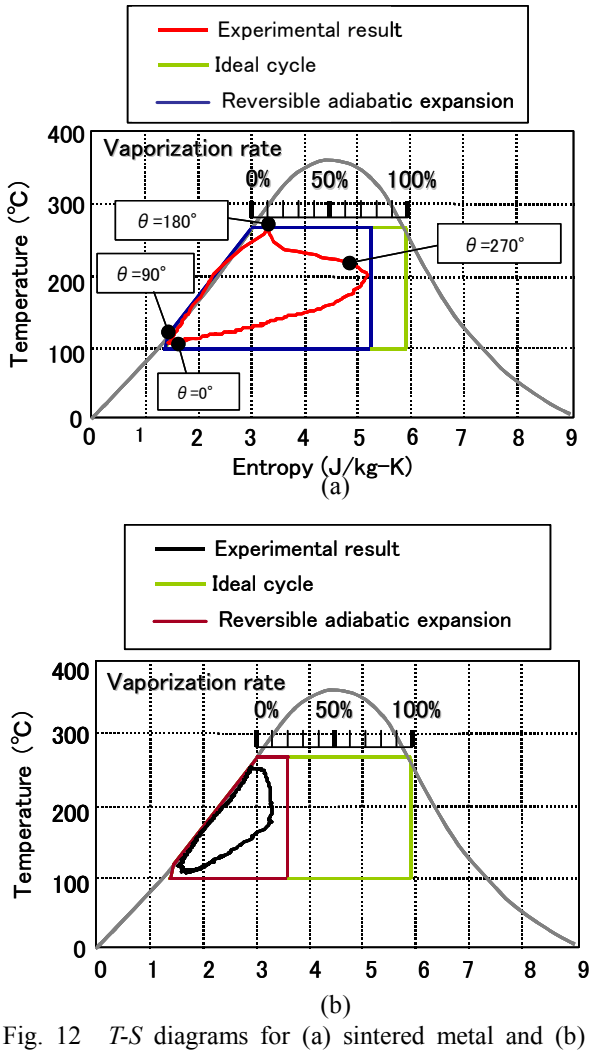


Fig. 12 *T-S* diagrams for (a) sintered metal and (b) hollow channel evaporators.

## SUMMARY

A novel liquid-piston steam engine which can achieve high efficiency as well as high reliability and low cost in the low temperature range is developed.. Liquid piston engine with sintered metal evaporator achieved a thermal efficiency of 12.7% at a heating temperature of 270 °C and a cooling temperature of 80 °C, which was approximately 40% of Carnot efficiency. This measured efficiency value is much higher than those of thermoelectric devices and thermoacoustic engines, whose efficiencies are less than 10% under the same condition. The developed liquid piston engine is thus expected to possess large possibility of recovering energy from waste heat.

## REFERENCES

1. Backhaus, S. & Swift, G. W., A thermoacoustic Stirling heat engine, *Nature*, 399, 335–338 (1999).
2. Saitoh, T., Yamada, N. & Wakashima S., Solar Rankine cycle system using scroll expander, *J. Env. Eng.*, 2, 708–719 (2007).
3. Peterson, G. P. & Chang, C. S., Two-phase heat dissipation utilizing porous channels of high conductivity material, *ASME J. Heat Transf.*, 120, 243–252 (1998).
4. Kutateladze, S. S., Heat Transfer in Condensation and Boiling, 2nd edn., US AEC Tech, (1952).